Supplementary information

Individual variability in brain representations of pain

Supplementary Information for

# INDIVIDUAL VARIABILITY IN BRAIN REPRESENTATIONS OF PAIN

Lada Kohoutová[1,2,3], Lauren Y. Atlas[4,5,6*], Christian Büchel[7], Jason T. Buhle[8],
Stephan Geuter[9,10], Marieke Jepma[11], Leonie Koban[12], Anjali Krishnan[13], Dong Hee Lee[1,2,3],
Sungwoo Lee[1,2,3], Mathieu Roy[14], Scott M. Schafer[15], Liane Schmidt[12], Tor D. Wager[16],
Choong-Wan Woo[1,2,3]

[1]Center for Neuroscience Imaging Research, Institute for Basic Science, South Korea [2]Department of Biomedical Engineering, Sungkyunkwan University, South Korea [3]Department of Intelligent Precision Healthcare Convergence, Sungkyunkwan University, Suwon, South Korea [4]National Center for Complementary and Integrative Health, National Institutes of Health, USA [5]National Institute on Drug Abuse, National Institutes of Health, USA [6]National Institute of Mental Health, National Institutes of Health, USA [7]Department of Systems Neuroscience, University Medical Centre Hamburg-Eppendorf, Hamburg, Germany [8]Department of Psychology, University of Southern California, USA [9]Department of Biostatistics, Johns Hopkins University, USA [10]Institute of Cognitive Science, University of Colorado Boulder, USA [11]Department of Psychology, University of Amsterdam, The Netherlands [12]Control-Interoception-Attention Team, Paris Brain Institute (ICM), INSERM, CNRS, Sorbonne University, France [13]Department of Psychology, Brooklyn College of the City University of New York, USA [14]Department of Psychology, McGill University, Montreal, QC, Canada [15]Department of Psychology and Neuroscience, University of Colorado Boulder, USA [16]Department of Psychological and Brain Sciences, Dartmouth College, USA

*The authors are alphabetically ordered except for the first and corresponding author.

This PDF file includes:

1. Supplementary Figures 1-5
2. Supplementary Tables 1-4
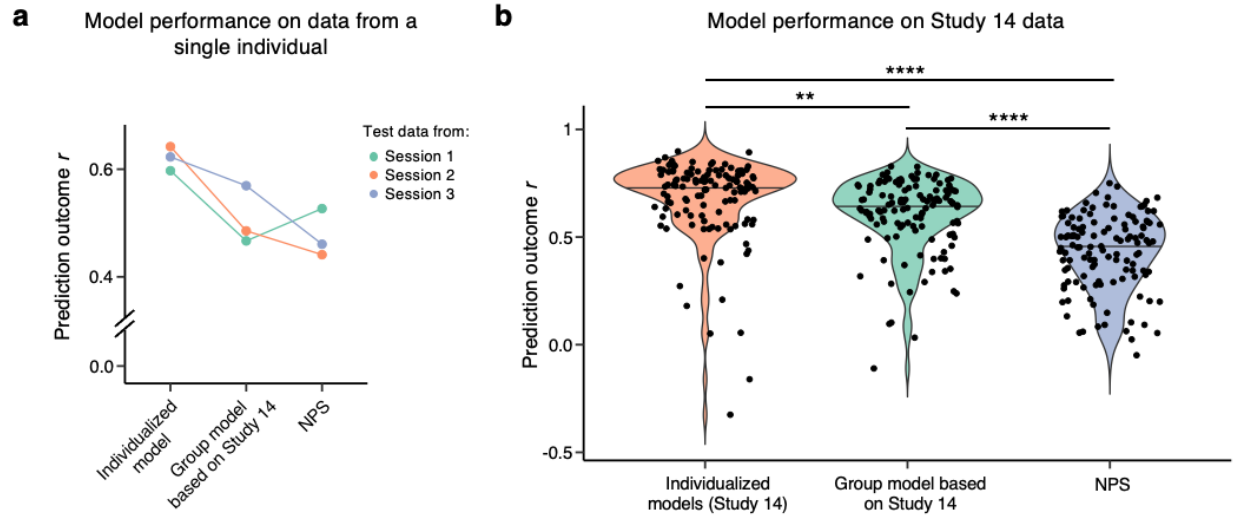
Supplementary Fig. 1. Comparison of the prediction performance of the individualized model and group-based models. (a) To compare the prediction performance of the individualized and group-based models, we performed a preliminary analysis with data of a single individual including four sessions of the same experiment as in Study 14. The individualized model was trained with one session of the four-session data. The remaining three sessions were used as testing data for the individualized model, a group model based on Study 14 and the Neurologic Pain Signature (NPS)[1]. The lines with different colors connect the testing results on the same session data. **(b)** We also compared the prediction performance of all individualized models from Study 14 (n = 124) that was obtained using 5-fold cross-validation in each model (orange), prediction performance of the group-based model built on Study 14 and Neurologic Pain Signature (NPS)[1] on data of each individual from Study 14 (n = 124). Again, the individualized models showed significantly higher performance than the group-based models. In a pairwise t-test, for individualized models vs. group-based model based on Study 14 p = 0.0015, for individualized models vs. NPS p = 9.64 ×10^{-23}, and for group-based model based on Study 14 vs. NPS p = 1.17 × 10^{-12}. All p-values are two-tailed and corrected for multiple comparisons using False Discovery Rate (FDR) correction. ** $p < 0.01$, **** $p < 0.0001$
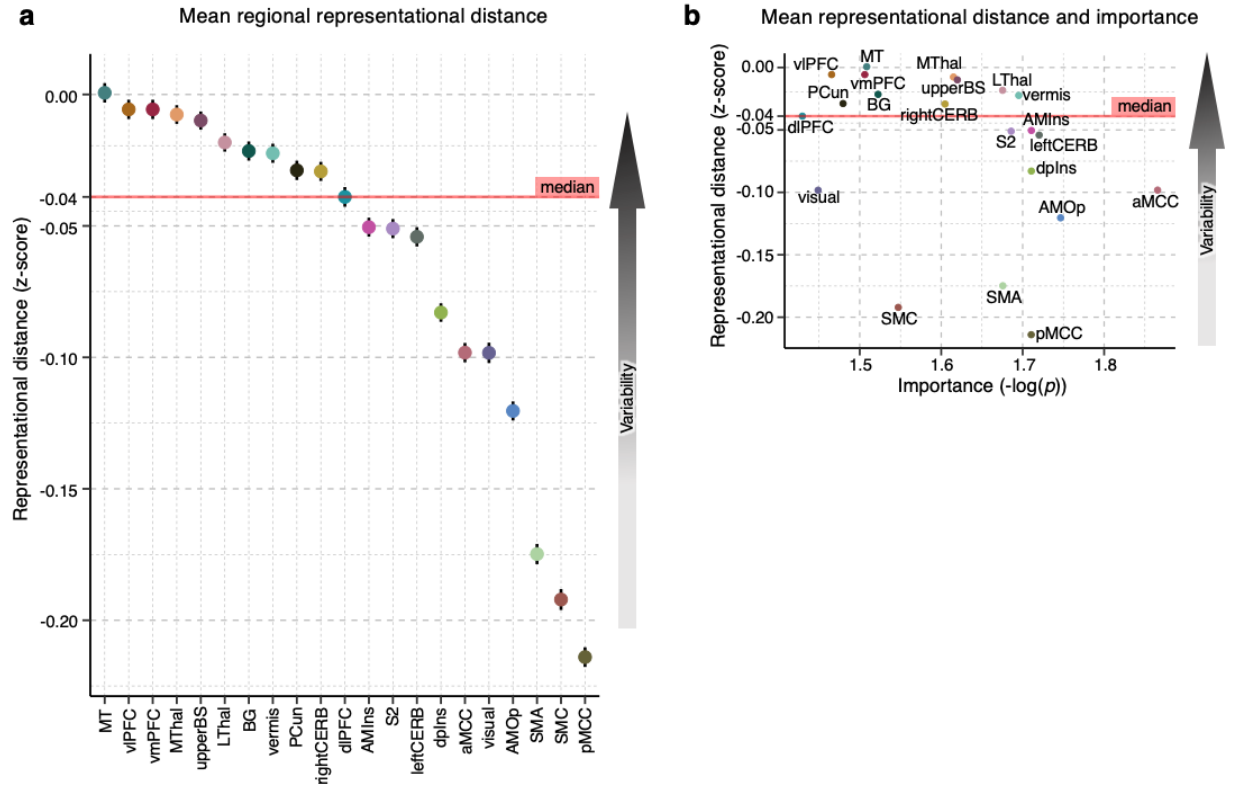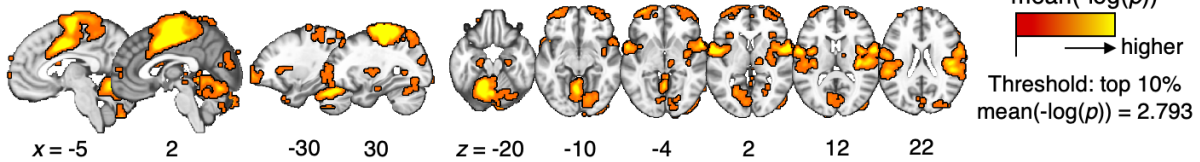
Supplementary Fig. 2. Mean representational distance without regressing out the region sizes. (a) The plot shows the mean representational distance (z-scores) and standard error of the mean for each region across all pair comparisons of individuals, i.e., $C(404, 2) = 81406$, before residualizing the region size. Higher representational distance values indicate higher pattern-level variability across people. **(b)** The scatter plot shows the relationship between the representational distance and mean importance measured by mean -log(p) (based on two-tailed p-values).

a Mean –log(*p*) map: discovery dataset (individualized maps)

mean(-log(*p*))

→ higher

Threshold: top 10%
mean(-log(*p*)) = 1.549
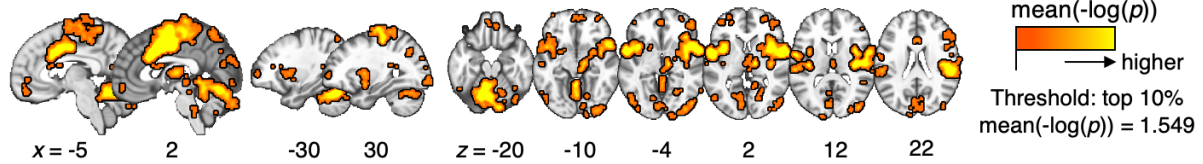
b Mean –log(*p*) map: replication dataset (individualized maps)

mean(-log(*p*))

→ higher

Threshold: top 10%
mean(-log(*p*)) = 2.793

c –log(*p*) map: group-based map built on replication dataset

-log(*p*)

→ higher

Threshold: top 10%
-log(*p*) = 8.510
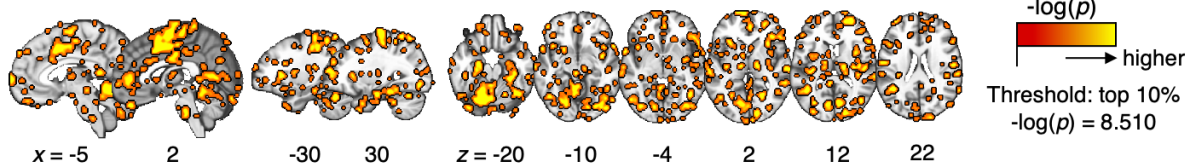
d Reverse inference map for pain from Neurosynth

Z-score

→ higher

Threshold:
q < 0.01, FDR
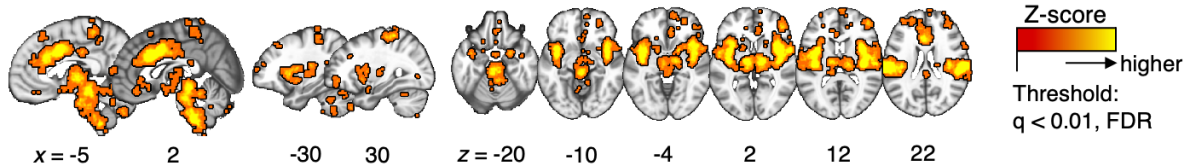
e Overlap of important voxels: **a** and **b**
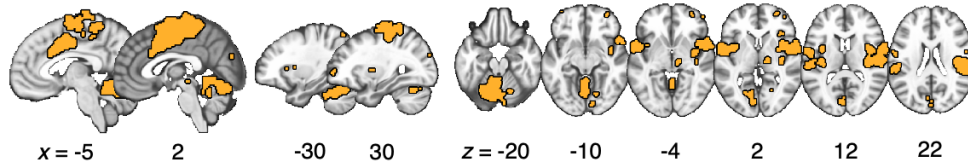
f Overlap of important voxels: **a** and **c**
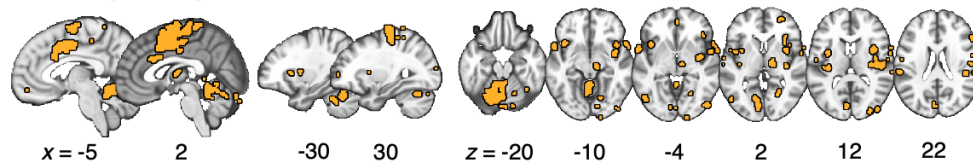
g Overlap of important voxels: **a** and **d**

Supplementary Fig. 3. Voxel importance maps and their overlaps. (a) Voxel importance map in the discovery dataset. **(b)** Voxel importance map in the replication dataset (Study 14). **(c)** Voxel importance map of the group-based model built on data from Study 14. To obtain the map, we ran the bootstrap tests with 5,000 samples, calculated the p-values and thresholded at top 10% of -log(p) = 8.510. **(d)** Reverse inference map for the term "pain" obtained from Neurosynth.org[2] thresholded at $q < 0.01$, FDR. **(e)** The binary overlap o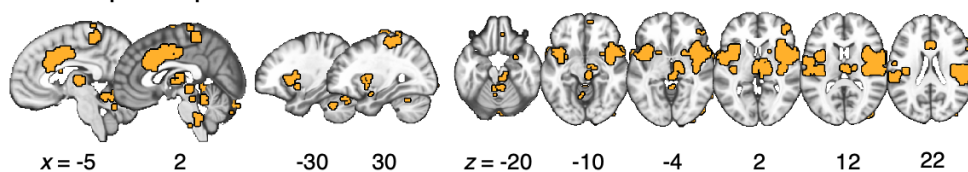f voxel importance maps shown in **Supplementary Fig. 9a** (individualized maps from the discovery dataset) and **Supplementary Fig. 9b** (individualized maps from Study 14). The two binarized voxel importance maps were correlated at $\phi = 0.502$, $p < 2.2 \times 10^{-16}$, suggesting high similarity between them. **(f)** The overlap of voxel importance maps shown in **Supplementary Fig. 9a** and **Supplementary Fig. 9c** (group-based map from Study 14). The correlation between the maps significant at $\phi = 0.186$, $p < 2.2 \times 10^{-16}$. **(g)** The overlap of voxel importance maps shown in **Supplementary Fig. 9a** and **Supplementary Fig. 9d** (Neurosynth map for the term "pain"). The maps were significantly correlated at $\phi = 0.287$, $p < 2.2 \times 10^{-16}$.
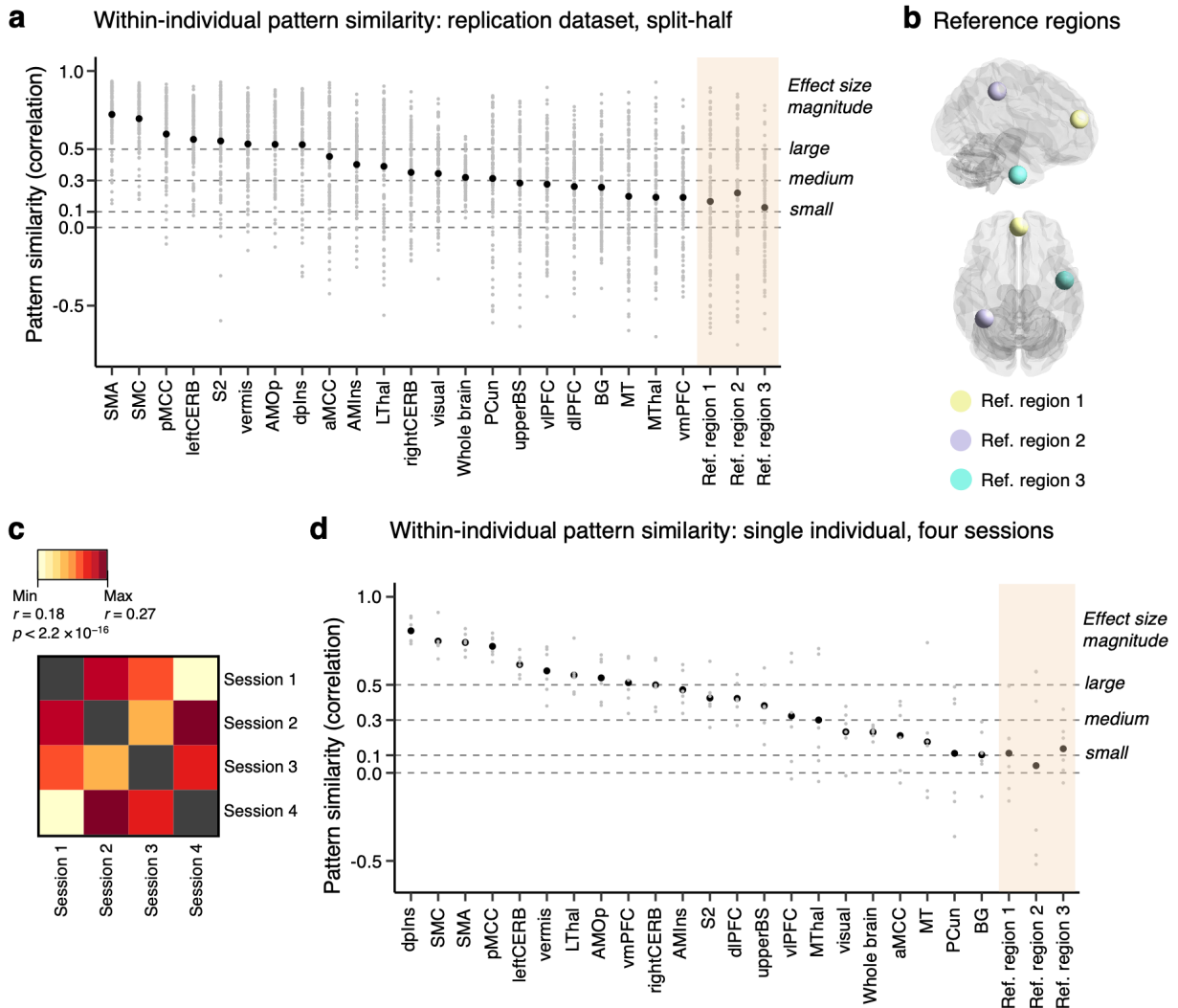
Supplementary Fig. 4. Within-individual reliability of pain predictive weights. (a) To evaluate the reliability of the predictive weights within individuals, we used the replication dataset and selected individuals with complete data of 96 trials ($n = 103$). In each individual, we split the trials into two folds (i.e., the first four and the last four runs) and trained an SVR model on each fold. We, then, assessed similarity of the predictive patterns of the whole brain, our 21 regions of interest, and three random regions as reference. The reference regions were defined as spheres (with 10-mm radius) around randomly selected points in areas that were not included as important pain-predictive regions in this study. The figure shows the mean within-individual pattern similarity (black points) as well as all values (gray points) measured by correlation. Most of the mean pattern similarity values showed medium-to-large correlations as evaluated by Cohen's guidelines[3], providing preliminary evidence for the reliability of the predictive patterns. **(b)** Glass brain visualization of the reference regions. **(c)** For further preliminary evaluation of the within-individual reliability, we used data of a single individual that were also used in

Supplementary Fig. 2. The heatmap shows the similarity measured by Pearson's correlation coefficient between whole-brain predictive patterns of the four sessions. **(d)** The plot depicts all values of the inter-session variability (small grey points) as well as their mean (large black points) in the whole brain and all regions of interest and reference regions. Based on the Cohen's guidelines, most of the regions manifested large or medium magnitude of correlation. On the other hand, the reference regions which were not found as important for pain prediction showed small magnitude of inter-session correlation. These results provide further preliminary support for reliability of predictive patterns within individuals.

a Comparison of subject-based dendrograms in region clusters

b Example of heterogeneity in subject clustering
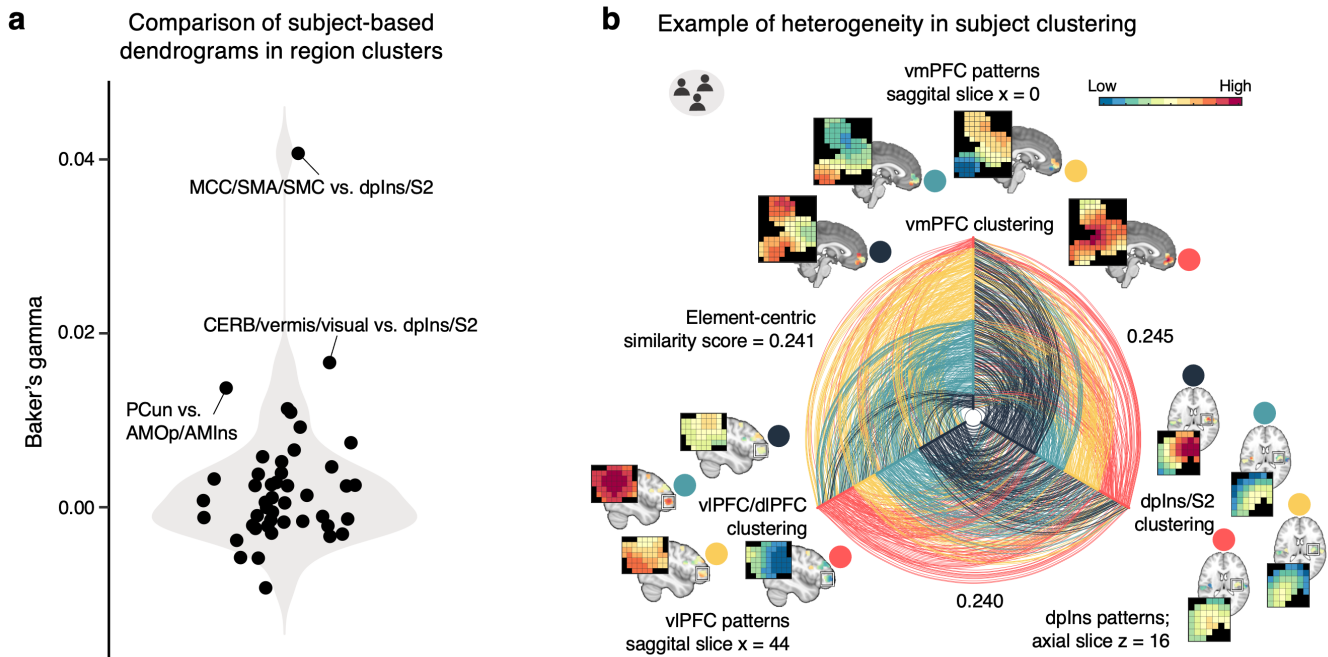
Supplementary Fig. 5. Clustering subjects. A potential future direction of analysis in which the region clusters identified in our study could be used is subtyping individuals or defining pain biotypes based on brain representations of pain in the clusters. Since we lacked detailed phenotype data of the participants, we could not fully interpret these results, but we conducted a simple *proof-of-concept* clustering analysis to establish a direction for the future work. **(a)** We built dendrograms using a hierarchical clustering algorithm with average linkage on the mean inter-individual representational dissimilarity matrices in all region clusters. Then, we compared the dendrograms of subjects using Baker's gamma. The violin plot shows that the resulting values were near zero, indicating that there was no statistically significant similarity of the dendrograms. This analysis suggests that subjects may constitute different subtypes across different brain regions. Therefore, lumping information from multiple brain regions to describe individuals can be costly. **(b)** We selected three region clusters, 1) dpIns and S2, 2) vlPFC and dlPFC, and 3) vmPFC, and clustered the subjects into four groups in each to further illustrate the heterogeneity of the subject subtypes in different regions. Each axis of the hive plot corresponds to each region cluster, and the points on the axes represent subjects colored by the cluster they belong to. The lines connect the same subjects in different clustering solutions (based on different brain regions) and are colored by the cluster membership in the previous clustering of the corresponding subject (counter-clockwise). The similarity between cluster solutions was evaluated with the element-centric similarity (EC) score[4], which ranges from 0 to 1, with 0 indicating completely different cluster membership and 1 indicating identical cluster membership profiles across individuals. The brain maps show the average patterns of predictive weights within each brain region across subjects within each subject cluster. This analysis also suggests that subjects may constitute different subtypes across different brain regions and clusters.

Supplementary Table 1. Demographics.

Study number	Sample size	Sex	Mean age in years (SD)	Previous publications
1	33	22 F	27.9 (9.0)	refs.[1,5]
2	28	10 F	25.2 (7.4)	ref.[6]
3	26	9 F	27.8	ref.[7]
4	50	27 F	25.1 (6.9)	ref.[8]
5	17	9 F	25.5	ref.[9]
6	29	16 F[a]	20.4 (3.3)[b]	ref.[10]
7	20	8 F	26.2 (6.7)	Unpublished
8	17[c]	11 F	24.7	ref.[11]
9	19	10 F	25.3 (9.3)	ref.[12]
10	26	11 F	28 (9.3)	ref.[13]
11	40	0 F	26	ref.[14]
12	40	20 F	Unknown[d]	Unpublished
13	59	31 F	20.8 (3.0)	ref.[15]
14	124	61 F	22.2 (2.7)	Unpublished

Note. [a]Sex of one participant is unknown. [b]Age of one participant is unknown [c]The original publication included 21 participants, but here we included only 17 participants' data due to the unsuccessful extraction of the single-trial data from 4 participants. [d]We were not able to extract the age information about this study, but the range should be comparable to other datasets collected at the University of Colorado Boulder (Studies 1, 2, 4, 9, 10) because the participants were recruited from the same subject pool.

Supplementary Table 2. Multiple regression in the discovery dataset with study-related parameters as predictors.

Regions	Scanner	Columbia vs. Boulder/Hamburg	Boulder vs. Hamburg	Body site	Stimulus duration	No. of trials	Cue	Adjusted R-squared	p-value
aMCC		-0.08**						0.02575	0.01512
AMIns		-0.04*						0.01877	0.04245
AMOp	0.06***	-0.07***		-0.05*				0.06365	2.44e-05
BG				-0.05***	0.01***			0.04861	0.000356
dlPFC								0.02599	0.01458
dpIns						-0.001*		0.004983	0.2546
leftCERB		-0.04*						0.02288	0.02329
LThal		-0.03*	0.02*	-0.03*	0.004*		0.03**	0.03453	0.003795
MT								-0.004984	0.6598
MThal			-0.02**			0.001***	-0.03***	0.05197	0.0001981
PCun	-0.03*		0.03*			-0.001*		0.02331	0.02186
pMCC				-0.12*	0.02**	0.002*		0.03932	0.001726
rightCERB				-0.03*	0.006**		0.02*	0.01836	0.04502
S2				-0.04*				0.001275	0.3796
SMA		-0.07*		-0.17***	0.02*	0.002*		0.08883	2.091e-07
SMC		-0.08**		-0.29***	0.04***	-0.002*	0.14***	0.1195	4.31e-10
upperBS					0.004*			0.01725	0.0527
vermis			0.02**	-0.02*				0.02577	0.01507
visual					0.01**		0.05*	0.04587	0.0005716
vlPFC				-0.04***	0.005**	-0.001*	0.03**	0.04443	0.0007305
vmPFC							-0.02*	0.03048	0.007251

Note. *$p < 0.05$, **$p < 0.01$, ***$p < 0.001$, uncorrected. The values in the variable columns show the significant predictors with their beta coefficients and levels of significance. Beta coefficients for non-significant predictors were omitted, but all variables were used in the model. Note that all results are uncorrected for the exploratory purpose, and if we use Bonferroni correction, the corrected threshold for significance becomes $p = 0.0024$.

The predictor variables were built as follows. In case of *scanner*, *body site* and *cue*, the variables were coded as 1 vs. -1 for 3 T vs. 1.5 T scanner, stimulation site on arm vs. leg, and presence vs. absence of cue. In *Columbia vs. Boulder/Hamburg*, studies performed at Columbia university were coded as -1, the rest as 0.5. In case of *Boulder vs. Hamburg*, the studies performed at University of Colorado in Boulder were coded as -1, study performed in Hamburg as 1, and the rest as 0. *Stimulus duration* and *no. of trials* were both continuous variables with the duration of stimulus in each study and number of trials available for each individual, respectively. All variables were mean-centered.

Supplementary Table 3. Task characteristics and stimulation parameters.

Study number (project name)	Stimulation site	Intensity levels	Temperature range (°C)	Duration (s)	Rating scale	Number of trials per person (mean number of trials used per person ± SD)	Other experimental manipulations
1 (bmrk3)	Arm	6 (fix)	44.3-49.3	12.5	0-200 VAS[a]	97 (45.5 ± 18.6)	Cognitive self-regulation to increase or decrease pain
2 (bmrk4)	Arm, foot	3 (fix)	46-48	11	0-100 LMS[b]	81 (74 ± 5.9)	Heat-predictive cues for low, medium and high
3 (nsf)	Arm	4 (cal)	PT/L/M/H	10	0-10 VAS[c]	48 (44.2 ± 3.2)	Masked emotional faces evenly crossed with temperature
4 (ie)	Arm	3 (fix)	46-48	11	0-100 VAS[d]	48 (42.1 ± 4.7)	Heat-predictive visual cues and placebo manipulation
5 (exp)	Arm	3 (cal)	L/M/H	10	0-10 VAS[c]	64 (61.1 ± 2.6)	Heat-predictive auditory cues
6 (ilcp)	Arm	2 (cal)	L/H	10	0-100 VAS[d]	64 (63 ± 1.3)	Perceived control (make choice vs. observe choice); expectation (80% vs. 50% low pain)
7 (app)	Arm	2 (cal)	L/M	20.16	0-100 VAS[e]	90 (75.8 ± 20.8)	Placebo manipulation and distracting cognitive tasks
8 (remi)	Arm	2 (cal)	L//H	10	0-8 VAS[f]	72 (68.2 ± 5.1)	Analgesic drug administration, analgesia expectancy, heat-predictive visual cues
9 (ie2)	Leg	2 (fix)	48, 49	1.8	0-100 VAS[d]	70 (67.7 ± 2.2)	Cues previously associated with high or low heat
10 (scebl)	Leg	3 (fix)	48, 49, 50	1.85	0-100 VAS[d]	96 (90 ± 3.5)	Social cues and heat-predictive visual cues
11 (placebo value)	Arm	4 (cal)	VAS 30, 50, 60, 80	20	0-100 VAS[g]	60 (59.4 ± 2.4)	Expectation and placebo manipulation
12 (levoderm)	Arm	2 (fix)	45.5, 46	20	0-100 VAS[d]	48 (46.3 ± 2.6)	Placebo conditioning manipulation with scheduled unblinding
13 (dpsp)	Arm	2 (cal)	L/H	15	1-5 Likert[h]	16 (15.6 ± 0.9)	Eye gaze fixation cross
14 (mpc)	Arm	6 (fix)	45, 45.5, 46, 46.5, 47, 47.5	12	0-1 gLMS[i]	96 (91.6 ± 10.6)	Pre-stimulus state manipulations by video watching

Note. Cal – temperature levels individually calibrated; fix – temperature levels same for all participants; [a] Pain or no pain decision followed by 0-100 VAS for warmth or pain rating. [b] 0 – no sensation; 1.4 – barely detectable; 6.1 – weak; 17.2 – moderate; 35.4 – strong; 53.3 – very strong; 100 – strongest imaginable sensation. [c] 0 – no sensation; 1 – non-painful warmth; 2 – low pain; 5 – moderate pain; 8 – maximum tolerable pain. [d] 0 – no pain; 100 – worst imaginable pain. [e] 0 – no pain; 100 – worst tolerable pain. [f] 0 – no sensation; 1 – nonpainful warmth; 2 – low pain; 5 – moderate pain; 8 – maximum tolerable pain. [g] 0 – no pain; 100 – unbearable pain. [h] 1 – not painful; 5 – very painful. [i] 0 – no pain; 1 – "I never want to experience this again in my life" [16]

Supplementary Table 4. Acquisition parameters.

Study number	Study location	Scanner details	Sequence parameters	Voxel size (mm³)	Acquisition parameters	Discarded volumes	Stimulus software	Analysis software
1 (bmrk3)	Columbia	3T Phillips Achieva TX	Seq. type = EPI TR = 2000 ms TE = 20 ms FOV = 224 mm Matrix = 64×64 Flip angle = 72°	$3.0 \times 3.0 \times 3.0$	42 Slices Interleaved SENSE = 1.5	4	E-prime	SPM8
2 (bmrk4)	CU Boulder	3T Siemens Tim Trio	Seq. type = EPI TR = 1300 ms TE = 25 ms FOV = 220 mm Matrix=64×64 Flip angle = 50°	$3.4 \times 3.4 \times 3.4$	26 Slices Interleaved iPAT = 2	6	Matlab	SPM8
3 (nsf)	Columbia	1.5T GE Signa TwinSpeed Excite HD	Seq. type = EPI TR = 2000 ms TE = 34 ms FOV = 224 mm Matrix = 64 × 64	$3.5 \times 3.5 \times 4.0$	29 Slices	5	E-prime	SPM5, SPM8
4 (ie)	CU Boulder	3T Siemens Tim Trio	Seq. type = EPI TR = 1300 ms TE = 25 ms FOV = 220 mm Matrix=64×64 Flip angle = 75°	$3.4 \times 3.4 \times 3.0$	26 Slices Interleaved iPAT = 2	6	E-prime	SPM8
5 (exp)	Columbia	1.5T GE Signa Twin Speed Excite HD	Seq. type = spiral TR = 2000 ms TE = 40 ms FOV = 224 mm Matrix = 64 × 64 Flip angle = 84°	$3.5 \times 3.5 \times 4.5$	24 Slices	5	E-prime	SPM5
6 (ilcp)	CU Boulder	3T Siemens Tim Trio	Seq. type = EPI TR = 1980 ms TE = 25 ms FOV = 220 mm Matrix=64×64 Flip angle = 75°	$3.4 \times 3.4 \times 3.0$	35 Slices Interleaved iPAT = 2	5	Matlab	SPM8
7 (app)	Columbia	3T Philips	Seq. type = EPI TR = 2000 ms TE = 20 ms FOV = 224 mm Flip angle = 72°	$3.0 \times 3.0 \times 3.0$	42 slices	4	E-prime	SPM5

8 (remi)	Columbia	1.5T GE Signa Twin Speed Excite HD	Seq. type = EPI TR = 2000 ms TE = 34 ms FOV = 224 mm Matrix = 64 $\times$ 64	3.5 $\times$ 3.5 $\times$ 4.0	28 slices	5	E-prime	SPM5
9 (ie2)	CU Boulder	3T Siemens Trio	Seq. type = EPI TR = 1300 ms TE = 25 ms FOV = 220 mm	3.4 $\times$ 3.4 $\times$ 3.0	26 slices	6	E-prime	SPM8
10 (scebl)	CU Boulder	3T Siemens Tim Trio	Seq. type = EPI TR = 1300 ms TE = 25 ms FOV = 220 mm Matrix = 64$\times$64 Flip angle = 50°	3.4 $\times$ 3.4 $\times$ 3.4	26 Slices Interleaved iPAT = 2	3	E-prime	SPM8
11 (placebovalue)	Hamburg	3T Siemens Tim Trio	Seq. type = EPI TR = 2580 ms TE = 26 ms FOV = 220 mm Flip angle = 80°	2 $\times$ 2 $\times$ 2	42 slices	4	Cogent	SPM8
12 (levo derm)	CU Boulder	3T Siemens Tim Trio	Seq. type = EPI TR = 1300 ms TE = 27 ms FOV, matrix, flip angle unknown	3 $\times$ 3 $\times$ 3	25 slices	6	E-prime	SPM8
13 (dpsp pain)	Columbia	1.5T GE Signa TwinSpeed Excite HD	Seq. type = spiral TR = 2000 ms TE = 40 ms FOV = 220 mm Flip angle = 84°	3.5 $\times$ 3.5 $\times$ 4.5	24 slices	4	E-prime	SPM8
14 (Replication dataset)	CNIR	3T Siemens Prisma	Seq. type = EPI TR = 460 ms TE = 2.34 ms FOV = 220 mm Matrix = 82$\times$82 Flip angle = 44°	2.7 $\times$ 2.7 $\times$ 2.7	56 slices	18	Matlab	SPM12, FSL, ICA-AROMA

Note. Columbia – Columbia University, New York, USA; CU Boulder – University of Colorado at Boulder, Colorado, USA; Hamburg – University Medical Center Hamburg-Eppendorf, Germany; CNIR– Center for Neuroscience Imaging Research, Sungkyunkwan University, South Korea

References

1   Wager, T. D. *et al.* An fMRI-Based Neurologic Signature of Physical Pain. *New Engl J Med* **368**, 1388-1397, doi:10.1056/NEJMoa1204471 (2013).

2   Yarkoni, T., Poldrack, R. A., Nichols, T. E., Van Essen, D. C. & Wager, T. D. Large-scale automated synthesis of human functional neuroimaging data. *Nat Methods* **8**, 665-U695, doi:10.1038/Nmeth.1635 (2011).

3   Cohen, J. *Statistical power analysis for the behavioral sciences*. 2nd edn, (L. Erlbaum Associates, 1988).

4   Gates, A. J., Wood, I. B., Hetrick, W. P. & Ahn, Y. Y. Element-centric clustering comparison unifies overlaps and hierarchy. *Sci Rep-Uk* **9**, doi:10.1038/s41598-019-44892-y (2019).

5   Woo, C. W., Roy, M., Buhle, J. T. & Wager, T. D. Distinct Brain Systems Mediate the Effects of Nociceptive Input and Self-Regulation on Pain. *Plos Biol* **13**, doi:10.1371/journal.pbio.1002036 (2015).

6   Krishnan, A. *et al.* Somatic and vicarious pain are represented by dissociable multivariate brain patterns. *Elife* **5**, doi:10.7554/eLife.15166 (2016).

7   Atlas, L. Y., Lindquist, M. A., Bolger, N. & Wager, T. D. Brain mediators of the effects of noxious heat on pain. *Pain* **155**, 1632-1648, doi:10.1016/j.pain.2014.05.015 (2014).

8   Roy, M. *et al.* Representation of aversive prediction errors in the human periaqueductal gray. *Nat Neurosci* **17**, 1607-1612, doi:10.1038/nn.3832 (2014).

9   Atlas, L. Y., Bolger, N., Lindquist, M. A. & Wager, T. D. Brain mediators of predictive cue effects on perceived pain. *J Neurosci* **30**, 12964-12977, doi:10.1523/JNEUROSCI.0057-10.2010 (2010).

10   Woo, C.-W. *et al.* Quantifying cerebral contributions to pain beyond nociception. *Nat Commun* **8** (2017).

11   Atlas, L. Y. *et al.* Dissociable Influences of Opiates and Expectations on Pain. *Journal of Neuroscience* **32**, 8053-8064, doi:10.1523/Jneurosci.0383-12.2012 (2012).

12   Jepma, M., Koban, L., van Doorn, J., Jones, M. & Wager, T. D. Behavioural and neural evidence for self-reinforcing expectancy effects on pain. *Nature Human Behaviour* **2**, 838-855, doi:10.1038/s41562-018-0455-8 (2018).

13   Koban, L., Jepma, M., López-Solà, M. & Wager, T. D. Different brain networks mediate the effects of social and conditioned expectations on pain. *Nat Commun* **10**, 4096, doi:10.1038/s41467-019-11934-y (2019).

14   Geuter, S., Eippert, F., Hindi Attar, C. & Buchel, C. Cortical and subcortical responses to high and low effective placebo treatments. *Neuroimage* **67**, 227-236, doi:10.1016/j.neuroimage.2012.11.029 (2013).

15   Woo, C.-W. *et al.* Separate neural representations for physical pain and social rejection. *Nat Commun* **5**, doi:10.1038/ncomms6380 (2014).

16   Bartoshuk, L. M. *et al.* Valid across-group comparisons with labeled scales: the gLMS versus magnitude matching. *Physiol Behav* **82**, 109-114, doi:10.1016/j.physbeh.2004.02.033 (2004).